Scattering Analysis of Bi-anisotropic Materials Using Fast Dipole Method

Deng Xiaoqiao(邓小乔)[1], *Gu Changqing*(顾长青)[2*], *Li Zhuo*(李茁)[2]

1. Department of Electronic Information, Jiangsu University of Science and Technology, Zhenjiang, 212003, P. R. China;
2. College of Electronic and Information Engineering, Nanjing University of Aeronautics and Astronautics, Nanjing, 210016, P. R. China

(Received 5 January 2013; revised 19 March 2013; accepted 22 April 2013)

Abstract: Electromagnetic scattering from inhomogeneous three-dimensional (3D) bi-anisotropic scatterers is formulated in terms of the volume integral equation (VIE) method. Based on the volume equivalence principle, the VIE is represented in terms of a pair of coupled bi-anisotropic polarized volume electric and magnetic flux densities. The VIE is solved using the method of moments (MoM) combined with tetrahedral mesh. Then the fast dipole method (FDM) based on the equivalent dipole method (EDM) is extended to analyze the scattering of bi-anisotropic media by solving the VIE. Finally, some numerical results are given to demonstrate the accuracy of the developed method for the scattering analysis of the bi-anisotropic media.

Key words: equivalent dipole method (EDM); fast dipole method (FDM); bi-anisotropic media; scattering

CLC number: TN011 **Document code**: A **Article ID**: 1005-1120(2014)03-0274-07

1 Introduction

Considerable attentions have been given to bi-anisotropic media in recent years because of their unique properties in affecting the behavior of electromagnetic fields[1-4]. As a kind of complex media, bi-anisotropic media incorporates large variety of media, such as chiral or bi-isotropic media, gyrotropic chiral media, Faraday chiral media, anisotropic media, gyrotropic media, and so on.

A number of numerical studies concerning bi-anisotropic materials and its scattering properties have been developed[5-13], such as finite-difference time-domain (FDTD) method[5], hybrid finite element boundary integral (FEBI) method[6], and method of moments (MoM)[7-9]. However, time-domain methods rely on the Z-transform of analytical expressions that describe the dispersion properties of a material. These analytical expressions are in many cases very difficult to be obtained. The disadvantage of FEBI is that the boundary element method (BEM) matrix is dense, which greatly limits the application of FEBI in solving electrically large problems. The MoM as one of the most popular approaches has been extensively adopted for solving arbitrarily shaped three-dimensional (3D) inhomogeneous anisotropic bodies. However, it is well known that the MoM usually results in a very large and dense matrix when applied to analyze electrically large objects. For the reason, some fast algorithms, such as the multilevel fast multipole algorithm[10, 11], precorrected-FFT algorithm[12], adaptive integral method (AIM)[13], equivalent dipole method (EDM)[14, 15], and fast dipole method (FDM)[16-18] are generally employed to reduce the memory requirement and speed up the solution process.

In this paper, the volume integral equations (VIE) is formulated for electromagnetic scattering by arbitrarily shaped complex bodies with in-

Foundation items: Supported by the National Natural Science Foundation of China (61071019); the Joint Funding Project of the Aerospace Science Foundation Office of China (2008ZA52006).

* **Corresponding author**: Gu Changqing, Professor, E-mail: gucq@nuaa.edu.cn.

homogeneous bi-anisotropic scatterer. Then the FDM based on the EDM is first extended to solve the VIE.

2 VIE Formulations for Bi-anisotropic Materials

The constitutive relations for bi-anisotropic materials can be written by the following constitutive relations

$$\boldsymbol{D}=\bar{\bar{\boldsymbol{\varepsilon}}}_r\varepsilon_0\cdot\boldsymbol{E}+\bar{\bar{\boldsymbol{\xi}}}\sqrt{\varepsilon_0\mu_0}\cdot\boldsymbol{H} \tag{1}$$

$$\boldsymbol{B}=\bar{\bar{\boldsymbol{\zeta}}}\sqrt{\varepsilon_0\mu_0}\cdot\boldsymbol{E}+\bar{\bar{\boldsymbol{\mu}}}_r\mu_0\cdot\boldsymbol{H} \tag{2}$$

where $\bar{\bar{\boldsymbol{\varepsilon}}}_r$ and $\bar{\bar{\boldsymbol{\mu}}}_r$ are the relative permittivity and permeability tensor, respectively; $\bar{\bar{\boldsymbol{\xi}}}$ and $\bar{\bar{\boldsymbol{\zeta}}}$ the magnetoelectric tensors. One of the fundamental properties of bi-anisotropic media is the cross-coupling between the electric and magnetic fields.

For bi-anisotropic materials, Eqs. (1,2) can also be rewritten by

$$\begin{bmatrix}\boldsymbol{E}\\ \boldsymbol{H}\end{bmatrix}=\begin{bmatrix}\bar{\bar{\boldsymbol{\alpha}}}_1 & \bar{\bar{\boldsymbol{\alpha}}}_2\\ \bar{\bar{\boldsymbol{\alpha}}}_3 & \bar{\bar{\boldsymbol{\alpha}}}_4\end{bmatrix}\begin{bmatrix}\boldsymbol{D}\\ \boldsymbol{B}\end{bmatrix} \tag{3}$$

in which

$$\begin{bmatrix}\bar{\bar{\boldsymbol{\alpha}}}_1 & \bar{\bar{\boldsymbol{\alpha}}}_2\\ \bar{\bar{\boldsymbol{\alpha}}}_3 & \bar{\bar{\boldsymbol{\alpha}}}_4\end{bmatrix}=\begin{bmatrix}\bar{\bar{\boldsymbol{\varepsilon}}} & \bar{\bar{\boldsymbol{\xi}}}'\\ \bar{\bar{\boldsymbol{\zeta}}}' & \bar{\bar{\boldsymbol{\mu}}}\end{bmatrix}^{-1} \tag{4}$$

where $\bar{\bar{\boldsymbol{\varepsilon}}}=\bar{\bar{\boldsymbol{\varepsilon}}}_r\varepsilon_0$, $\bar{\bar{\boldsymbol{\mu}}}=\bar{\bar{\boldsymbol{\mu}}}_r\mu_0$, $\bar{\bar{\boldsymbol{\xi}}}'=\bar{\bar{\boldsymbol{\xi}}}\sqrt{\varepsilon_0\mu_0}$, and $\bar{\bar{\boldsymbol{\zeta}}}'=\bar{\bar{\boldsymbol{\xi}}}\sqrt{\varepsilon_0\mu_0}$. Based on the volume equivalence principle, the equivalent electric and magnetic polarization currents $\boldsymbol{J}_v(r)$ and $\boldsymbol{M}_v(r)$ can be expressed by

$$\begin{bmatrix}\boldsymbol{J}_v\\ \boldsymbol{M}_v\end{bmatrix}=\mathrm{j}\omega\begin{bmatrix}\bar{\bar{\boldsymbol{\beta}}}_1 & \bar{\bar{\boldsymbol{\beta}}}_2\\ \bar{\bar{\boldsymbol{\beta}}}_3 & \bar{\bar{\boldsymbol{\beta}}}_4\end{bmatrix}\begin{bmatrix}\boldsymbol{D}\\ \boldsymbol{B}\end{bmatrix} \tag{5}$$

where

$$\bar{\bar{\boldsymbol{\beta}}}_1=(\bar{\bar{\boldsymbol{\varepsilon}}}-\varepsilon_0\bar{\bar{\boldsymbol{I}}})\cdot\bar{\bar{\boldsymbol{\alpha}}}_1+\bar{\bar{\boldsymbol{\xi}}}'\cdot\bar{\bar{\boldsymbol{\alpha}}}_3 \tag{6}$$

$$\bar{\bar{\boldsymbol{\beta}}}_2=(\bar{\bar{\boldsymbol{\varepsilon}}}-\varepsilon_0\bar{\bar{\boldsymbol{I}}})\cdot\bar{\bar{\boldsymbol{\alpha}}}_2+\bar{\bar{\boldsymbol{\xi}}}'\cdot\bar{\bar{\boldsymbol{\alpha}}}_4 \tag{7}$$

$$\bar{\bar{\boldsymbol{\beta}}}_3=(\bar{\bar{\boldsymbol{\mu}}}-\mu_0\bar{\bar{\boldsymbol{I}}})\cdot\bar{\bar{\boldsymbol{\alpha}}}_3+\bar{\bar{\boldsymbol{\zeta}}}'\cdot\bar{\bar{\boldsymbol{\alpha}}}_1 \tag{8}$$

$$\bar{\bar{\boldsymbol{\beta}}}_4=(\bar{\bar{\boldsymbol{\mu}}}-\mu_0\bar{\bar{\boldsymbol{I}}})\cdot\bar{\bar{\boldsymbol{\alpha}}}_4+\bar{\bar{\boldsymbol{\zeta}}}'\cdot\bar{\bar{\boldsymbol{\alpha}}}_2 \tag{9}$$

The total fields represented by a sum of the incident and scattered fields can be obtained by

$$\boldsymbol{E}=\boldsymbol{E}^i-\mathrm{j}\omega\boldsymbol{A}_v^e(\boldsymbol{r})-\nabla\varphi_v^e(\boldsymbol{r})-\frac{1}{\varepsilon_0}\nabla\times\boldsymbol{A}_v^m(\boldsymbol{r})\quad \boldsymbol{r}\in V \tag{10}$$

$$\boldsymbol{H}=\boldsymbol{H}^i-\mathrm{j}\omega\boldsymbol{A}_v^m(\boldsymbol{r})-\nabla\varphi_v^m(\boldsymbol{r})+\frac{1}{\mu_0}\nabla\times\boldsymbol{A}_v^e(\boldsymbol{r})\quad \boldsymbol{r}\in V \tag{11}$$

where

$$\boldsymbol{A}_v^e(\boldsymbol{r})=\mu_0\int_v\boldsymbol{J}_v(\boldsymbol{r}')G_0(\boldsymbol{r},\boldsymbol{r}')\mathrm{d}v' \tag{12}$$

$$\boldsymbol{A}_v^m(\boldsymbol{r})=\varepsilon_0\int_v\boldsymbol{M}_v(\boldsymbol{r}')G_0(\boldsymbol{r},\boldsymbol{r}')\mathrm{d}v' \tag{13}$$

$$\varphi_v^e(\boldsymbol{r})=-\frac{1}{\mathrm{j}\omega\varepsilon_0}\int_v\nabla'\cdot\boldsymbol{J}_v(\boldsymbol{r}')G_0(\boldsymbol{r},\boldsymbol{r}')\mathrm{d}v' \tag{14}$$

$$\varphi_v^m(r)=-\frac{1}{\mathrm{j}\omega\mu_0}\int_v\nabla'\cdot\boldsymbol{M}_v(\boldsymbol{r}')G_0(\boldsymbol{r},\boldsymbol{r}')\mathrm{d}v' \tag{15}$$

where $G_0(\boldsymbol{r},\boldsymbol{r}')$ is the free space Green's function.

3 MoM Matrix Equation

The inhomogeneous bi-anisotropic objects are divided into tetrahedrons. For each face of the tetrahedron, we assign a basis function. Then both the electric flux density $\boldsymbol{D}$ and magnetic flux density $\boldsymbol{B}$ are expanded by Schaubert-Wilton-Glisson (SWG) vector basis functions[19], namely

$$\boldsymbol{B}(\boldsymbol{r})=\sum_{n=1}^{N}B_n\boldsymbol{f}_{vn}(\boldsymbol{r}) \tag{16}$$

$$\boldsymbol{D}(\boldsymbol{r})=\sum_{n=1}^{N}D_n\boldsymbol{f}_{vn}(\boldsymbol{r}) \tag{17}$$

where N is the total number of faces of the tetrahedral meshes. D_n and B_n are the unknown coefficients to be determined. $\boldsymbol{f}_{vn}$ denotes the nth volume basis function defined in two adjoining tetrahedrons in the volume meshes associated with common face n.

Using the Galerkin's method, the integral equations are converted into a matrix equation, and can be formally written as

$$\begin{bmatrix}\boldsymbol{Z}^{ee} & \boldsymbol{Z}^{em}\\ \boldsymbol{Z}^{me} & \boldsymbol{Z}^{mm}\end{bmatrix}\begin{bmatrix}\boldsymbol{I}^e\\ \boldsymbol{I}^m\end{bmatrix}=\begin{bmatrix}\boldsymbol{V}^e\\ \boldsymbol{V}^m\end{bmatrix} \tag{18}$$

where the elements of the block impendance matrices are

$$\boldsymbol{Z}_{mn}^{ee}=\int_{T_m}\boldsymbol{f}_{vm}(\boldsymbol{r})\cdot(\bar{\bar{\boldsymbol{\alpha}}}_1\cdot\boldsymbol{f}_{vn}(\boldsymbol{r}))\,\mathrm{d}v-\omega^2\mu_0\int_{T_m}\boldsymbol{f}_{vm}(\boldsymbol{r})\cdot\int_{T_n}G(\boldsymbol{r},\boldsymbol{r}')(\bar{\bar{\boldsymbol{\beta}}}_1\cdot\boldsymbol{f}_{vn}(\boldsymbol{r}))\mathrm{d}v'\mathrm{d}v+\frac{1}{\varepsilon_0}\int_{T_m}\nabla\cdot\boldsymbol{f}_{vm}(\boldsymbol{r})\int_{T_n}G(\boldsymbol{r},\boldsymbol{r}')\nabla\cdot(\bar{\bar{\boldsymbol{\beta}}}_1\cdot\boldsymbol{f}_{vn}(\boldsymbol{r}))\,\mathrm{d}v'\mathrm{d}v+$$

$$\mathrm{j}\omega\int_{T_m} \boldsymbol{f}_{vm} \cdot \int_{T_n} \nabla G(\boldsymbol{r},\boldsymbol{r}') \times (\bar{\bar{\boldsymbol{\beta}}}_3 \cdot \boldsymbol{f}_{vn})\,\mathrm{d}v'\mathrm{d}v \tag{19}$$

$$\begin{aligned}\boldsymbol{Z}^{em}_{mn} = &\int_{T_m} \boldsymbol{f}_{vm}(\boldsymbol{r}) \cdot (\bar{\bar{\boldsymbol{\alpha}}}_2 \cdot \boldsymbol{f}_{vn}(\boldsymbol{r}))\,\mathrm{d}v - \\ &\omega^2\mu_0\int_{T_m} \boldsymbol{f}_{vm}(\boldsymbol{r}) \cdot \int_{T_n} G(\boldsymbol{r},\boldsymbol{r}')(\bar{\bar{\boldsymbol{\beta}}}_2 \cdot \\ &\boldsymbol{f}_{vn}(\boldsymbol{r}))\mathrm{d}v'\mathrm{d}v + \\ &\frac{1}{\varepsilon_0}\int_{T_m} \nabla \cdot \boldsymbol{f}_{vm}(\boldsymbol{r})\int_{T_n} G(\boldsymbol{r},\boldsymbol{r}')\nabla \cdot \\ &(\bar{\bar{\boldsymbol{\beta}}}_2 \cdot \boldsymbol{f}_{vn}(\boldsymbol{r}))\,\mathrm{d}v'\mathrm{d}v + \\ &\mathrm{j}\omega\int_{T_m} \boldsymbol{f}_{vm} \cdot \int_{T_n} \nabla G(\boldsymbol{r},\boldsymbol{r}') \times (\bar{\bar{\boldsymbol{\beta}}}_4 \cdot \boldsymbol{f}_{vn})\,\mathrm{d}v'\mathrm{d}v\end{aligned} \tag{20}$$

$$\begin{aligned}\boldsymbol{Z}^{me}_{mn} = &\int_{T_m} \boldsymbol{f}_{vm}(\boldsymbol{r}) \cdot (\bar{\bar{\boldsymbol{\alpha}}}_3 \cdot \boldsymbol{f}_{vn}(\boldsymbol{r}))\,\mathrm{d}v - \\ &\omega^2\varepsilon_0\int_{T_m} \boldsymbol{f}_{vm}(\boldsymbol{r}) \cdot \int_{T_n} G(\boldsymbol{r},\boldsymbol{r}')(\bar{\bar{\boldsymbol{\beta}}}_3 \cdot \\ &\boldsymbol{f}_{vn}(\boldsymbol{r}))\mathrm{d}v'\mathrm{d}v + \\ &\frac{1}{\mu_0}\int_{T_m} \nabla \cdot \boldsymbol{f}_{vm}(\boldsymbol{r})\int_{T_n} G(\boldsymbol{r},\boldsymbol{r})\nabla \cdot (\bar{\bar{\boldsymbol{\beta}}}_3 \cdot \\ &\boldsymbol{f}_{vn}(\boldsymbol{r}))\mathrm{d}v'\mathrm{d}v - \\ &\mathrm{j}\omega\int_{T_m} \boldsymbol{f}_{vm} \cdot \int_{T_n} \nabla G(\boldsymbol{r},\boldsymbol{r}') \times (\bar{\bar{\boldsymbol{\beta}}}_1 \cdot \boldsymbol{f}_{vn})\,\mathrm{d}v'\mathrm{d}v\end{aligned} \tag{21}$$

$$\begin{aligned}\boldsymbol{Z}^{mm}_{mn} = &\int_{T_m} \boldsymbol{f}_{vm}(\boldsymbol{r}) \cdot (\bar{\bar{\boldsymbol{\alpha}}}_4 \cdot \boldsymbol{f}_{vn}(\boldsymbol{r}))\,\mathrm{d}v - \\ &\omega^2\varepsilon_0\int_{T_m} \boldsymbol{f}_{vm}(\boldsymbol{r}) \cdot \int_{T_n} G(\boldsymbol{r},\boldsymbol{r}')(\bar{\bar{\boldsymbol{\beta}}}_4 \cdot \\ &\boldsymbol{f}_{vn}(\boldsymbol{r}))\mathrm{d}v'\mathrm{d}v + \\ &\frac{1}{\mu_0}\int_{T_m} \nabla \cdot \boldsymbol{f}_{vm}(\boldsymbol{r})\int_{T_n} G(\boldsymbol{r},\boldsymbol{r}')\nabla' \cdot \\ &(\bar{\bar{\boldsymbol{\beta}}}_4 \cdot \boldsymbol{f}_{vn}(\boldsymbol{r}))\,\mathrm{d}v'\mathrm{d}v - \\ &\mathrm{j}\omega\int_{T_m} \boldsymbol{f}_{vm} \cdot \int_{T_n} \nabla G(\boldsymbol{r},\boldsymbol{r}') \times (\bar{\bar{\boldsymbol{\beta}}}_2 \cdot \boldsymbol{f}_{vn})\,\mathrm{d}v'\mathrm{d}v\end{aligned} \tag{22}$$

4 FDM for Bi-anisotropic Materials

The FDM is an efficient way to solve the VIE, which is based on the EDM. In the EDM, each SWG element can be approximated as an infinitely small dipole with an equivalent moment. Referring to Refs. [14,15], the nth volume dipole moment $\boldsymbol{m}_{\mathrm{in}}$ can be represented as

$$\boldsymbol{m}_{\mathrm{in}} = a_n\bar{\bar{\boldsymbol{\beta}}}^{+}_{\mathrm{in}}(\boldsymbol{r}) \cdot (\boldsymbol{r}^{c}_{ns} - \boldsymbol{r}^{c+}_{n}) + a_n\bar{\bar{\boldsymbol{\beta}}}^{-}_{\mathrm{in}}(\boldsymbol{r}) \cdot (\boldsymbol{r}^{c-}_{n} - \boldsymbol{r}^{c}_{ns}) \quad i=1,2,3,4 \tag{23}$$

where $\boldsymbol{r}^{c\pm}_n$ are the position vector of the centroid of $T^{\pm}_n$ and $\boldsymbol{r}^{c}_{ns}$ is the position vector of the centroid of the common face of the $T^{\pm}_n$. a_n is the area of the nth common face associated with $T^{\pm}_n$. The impedance matrix elements in Eqs. (19—22) can be calculated by the EDM

$$\boldsymbol{Z}^{ee}_{mn} = \mathrm{j}k\eta\boldsymbol{m}'_m \cdot \bar{\boldsymbol{G}}(\boldsymbol{R}) \cdot \boldsymbol{m}_{1n} - \mathrm{j}k\boldsymbol{m}'_m \cdot \boldsymbol{G}(\boldsymbol{R}) \times \boldsymbol{m}_{3n} \tag{24}$$

$$\boldsymbol{Z}^{em}_{mn} = \mathrm{j}k\eta\boldsymbol{m}'_m \cdot \bar{\boldsymbol{G}}(\boldsymbol{R}) \cdot \boldsymbol{m}_{2n} - \mathrm{j}k\boldsymbol{m}'_m \cdot \boldsymbol{G}(\boldsymbol{R}) \times \boldsymbol{m}_{4n} \tag{25}$$

$$\boldsymbol{Z}^{me}_{mn} = \frac{\mathrm{j}k}{\eta}\boldsymbol{m}'_m \cdot \bar{\boldsymbol{G}}(\boldsymbol{R}) \cdot \boldsymbol{m}_{3n} + \mathrm{j}k\boldsymbol{m}_m \cdot \boldsymbol{G}(\boldsymbol{R}) \times \boldsymbol{m}_{1n} \tag{26}$$

$$\boldsymbol{Z}^{mm}_{mn} = \frac{\mathrm{j}k}{\eta}\boldsymbol{m}'_m \cdot \bar{\boldsymbol{G}}(\boldsymbol{R}) \cdot \boldsymbol{m}_{4n} + \mathrm{j}k\boldsymbol{m}'_m \cdot \boldsymbol{G}(\boldsymbol{R}) \times \boldsymbol{m}_{2n} \tag{27}$$

where

$$\bar{\boldsymbol{G}}(\boldsymbol{R}) = \frac{\mathrm{e}^{-\mathrm{j}kR}}{4\pi R}\left[\bar{\boldsymbol{I}}\left(1 + \frac{1}{\mathrm{j}kR} + \frac{1}{(\mathrm{j}kR)^2}\right) - \hat{\boldsymbol{R}}\hat{\boldsymbol{R}}\left(1 + \frac{3}{\mathrm{j}kR} + \frac{3}{(\mathrm{j}kR)^2}\right)\right] \tag{28}$$

$$\boldsymbol{G}(\boldsymbol{R}) = \frac{\mathrm{e}^{-\mathrm{j}kR}}{4\pi R}\left(1 + \frac{1}{\mathrm{j}kR}\right)\hat{\boldsymbol{R}} \tag{29}$$

$$\boldsymbol{m}'_m = a_m(\boldsymbol{r}^{c-}_m - \boldsymbol{r}^{c+}_m) \tag{30}$$

In Eqs. (28,29), $\boldsymbol{R} = \boldsymbol{r}_m - \boldsymbol{r}_n$, $R = |\boldsymbol{R}|$, $\hat{\boldsymbol{R}} = \boldsymbol{R}/R$. In addition, $\boldsymbol{r}_n = \frac{(\boldsymbol{r}^{c-}_n + \boldsymbol{r}^{c+}_n)}{2}$ and $\boldsymbol{r}_m = \frac{(\boldsymbol{r}^{c-}_m + \boldsymbol{r}^{c+}_m)}{2}$. $\boldsymbol{r}^{c\pm}_n$ ($\boldsymbol{r}^{c\pm}_m$) are the position vector of the centroid of $T^{\pm}_n$ ($T^{\pm}_m$). According to Refs. [14,15], the EDM can be applied when the distance between the source and the field dipole is greater than $0.15\lambda_g$ (λ_g is the wavelength in dielectric). It should be noted that λ_g is the maximum wavelength in dielectric when the medium is inhomogeneous.

In Refs. [16,18], the FDM is developed to efficiently calculate the interactions between far groups. Here, we use the number of interval groups $D(i,j)$ between group i and group j to decide if the two groups are near-group pair or far-group pair. $D(i,j) = \max\{|x_i - x_j|, |y_i - y_j|, |z_i - z_j|\}/d$, where (x_i, y_i, z_i) and (x_j, y_j, z_j) are the coordinates of the centroid of group i and group j respectively, and d is the side length of the group. For example, if $D(i,j) > D_b$, group i and group j are the far-group pair, where $D_b \geqslant 1$ is a given integer. And D_b can be used to control the accuracy of the FDM. Generally, the criterion $D_b = 3$ for the FDM usually can give good RCS solutions when the size of groups is smaller than 0.5λ. In the paper, D_b is taken as 1 to save memory requirements.

In order to describe how the FDM works for dielectric and magnetic materials, we consider two dipoles m and n, which belong to groups j and i, respectively, and suppose the two groups are a far-group pair. The distance between the two dipoles can be written as $\boldsymbol{R}=\boldsymbol{r}_m-\boldsymbol{r}_n=\boldsymbol{r}_{ji}+\boldsymbol{r}_{mj}+\boldsymbol{r}_{ni}$, where $\boldsymbol{r}_{ji}=\boldsymbol{r}_{o_j}-\boldsymbol{r}_{o_i}$, $\boldsymbol{r}_{mj}=\boldsymbol{r}_m-\boldsymbol{r}_{o_j}$, $\boldsymbol{r}_{ni}=\boldsymbol{r}_n-\boldsymbol{r}_{o_i}$, $\boldsymbol{r}_{o_j}$ and $\boldsymbol{r}_{o_i}$ are the center vector of the groups. According to Ref. [17], R^α in Eqs. (28, 29) can be expanded using Taylor series approximately

$$R^\alpha=|\boldsymbol{r}_{ji}+\boldsymbol{r}_{mj}+\boldsymbol{r}_{ni}|^\alpha=r_{ji}^\alpha\left[1+\left(\frac{2\hat{\boldsymbol{r}}_{ji}\cdot\boldsymbol{r}_{mj}}{r_{ji}}+\frac{r_{mj}^2}{r_{ji}^2}\right)+\left(\frac{2\hat{\boldsymbol{r}}_{ij}\cdot\boldsymbol{r}_{ni}}{r_{ij}}+\frac{r_{ni}^2}{r_{ij}^2}\right)-\frac{2\boldsymbol{r}_{mj}\cdot\boldsymbol{r}_{ni}}{r_{ji}^2}\right]^{\frac{\alpha}{2}}\approx R_m^{(\alpha)}+R_n^{(\alpha)} \tag{31}$$

where

$$R_m^{(\alpha)}=r_{ji}^\alpha\left[\frac{1}{2}+\alpha\left(\frac{\hat{\boldsymbol{r}}_{ji}\cdot\boldsymbol{r}_{mj}}{r_{ji}}+\frac{r_{mj}^2+(\alpha-2)(\hat{\boldsymbol{r}}_{ji}\cdot\boldsymbol{r}_{mj})^2}{2r_{ji}^2}\right)\right] \tag{32}$$

$$R_n^{(\alpha)}=r_{ij}^\alpha\left[\frac{1}{2}+\alpha\left(\frac{\hat{\boldsymbol{r}}_{ij}\cdot\boldsymbol{r}_{ni}}{r_{ij}}+\frac{r_{ni}^2+(\alpha-2)(\hat{\boldsymbol{r}}_{ij}\cdot\boldsymbol{r}_{ni})^2}{2r_{ij}^2}\right)\right] \tag{33}$$

And $\hat{\boldsymbol{R}}\hat{\boldsymbol{R}}$ can be approximated as

$$\hat{\boldsymbol{R}}\hat{\boldsymbol{R}}\approx\overline{\boldsymbol{T}}_m+\overline{\boldsymbol{T}}_n \tag{34}$$

where

$$\overline{\boldsymbol{T}}_m=\frac{1}{r_{ji}^2}\left[\frac{1}{2}\boldsymbol{r}_{ji}\boldsymbol{r}_{ji}+\boldsymbol{s}_m\boldsymbol{r}_{ji}+\boldsymbol{r}_{ji}\boldsymbol{s}_m\right] \tag{35}$$

$$\overline{\boldsymbol{T}}_n=\frac{1}{r_{ij}^2}\left[\frac{1}{2}\boldsymbol{r}_{ij}\boldsymbol{r}_{ij}+\boldsymbol{s}_n\boldsymbol{r}_{ij}+\boldsymbol{r}_{ij}\boldsymbol{s}_n\right] \tag{36}$$

$$\boldsymbol{s}_m=\boldsymbol{r}_{mj}-\boldsymbol{r}_{mj}\cdot\hat{\boldsymbol{r}}_{ji}\hat{\boldsymbol{r}}_{ji} \tag{37}$$

$$\boldsymbol{s}_n=\boldsymbol{r}_{ni}-\boldsymbol{r}_{ni}\cdot\hat{\boldsymbol{r}}_{ij}\hat{\boldsymbol{r}}_{ij} \tag{38}$$

Then substituting Eqs. (31, 34) into Eqs. (28, 29), the formulations of FDM for electromagnetic materials can be obtained.

Now we consider how to use the FDM to calculate the interactions among the equivalent electric or magnetic dipoles in group i and group j. The effect of all the electric and magnetic dipoles in group i on the mth electric dipoles in the group j can be expressed as

$$\sum_{n\in i}(\boldsymbol{Z}_{mn}^{ee}\boldsymbol{I}_n^e+\boldsymbol{Z}_{mn}^{em}\boldsymbol{I}_n^m)\approx \mathrm{j}k\eta\boldsymbol{m}'_m\cdot\left[\sum_{n=1}^{N_v}\overline{\boldsymbol{G}}(\boldsymbol{R})\cdot(\boldsymbol{m}_{1n}\boldsymbol{I}_n^e+\boldsymbol{m}_{2n}\boldsymbol{I}_n^m)-\frac{1}{\eta}\sum_{n=1}^{N_v}\boldsymbol{G}(\boldsymbol{R})\times(\boldsymbol{m}_{3n}\boldsymbol{I}_n^e+\boldsymbol{m}_{4n}\boldsymbol{I}_n^m)\right] \tag{39}$$

In a similar way, the effect of all the electric and magnetic dipoles in group i on the mth magnetic dipoles in the group j can be expressed as

$$\sum_{n\in i}(\boldsymbol{Z}_{mn}^{me}\boldsymbol{I}_n^e+\boldsymbol{Z}_{mn}^{mm}\boldsymbol{I}_n^m)\approx \mathrm{j}k\boldsymbol{m}'_m\cdot\left[\sum_{n=1}^{N_v}\boldsymbol{G}(\boldsymbol{R})\times(\boldsymbol{m}_{1n}\boldsymbol{I}_n^e+\boldsymbol{m}_{2n}\boldsymbol{I}_n^m)+\frac{1}{\eta}\sum_{n=1}^{N_v}\overline{\boldsymbol{G}}(\boldsymbol{R})\cdot(\boldsymbol{m}_{3n}\boldsymbol{I}_n^e+\boldsymbol{m}_{4n}\boldsymbol{I}_n^m)\right] \tag{40}$$

In the FDM, the calculation remains the same as in the MoM/EDM procedure for near-neighbor matrix elements. The calculation of the far-field interaction groups is significantly accelerated by the processes of aggregation-translation-disaggregation. According to Refs. [16 − 18], the complexity of interactions between two far groups such as group i and j is reduced from $O(N_iN_j)$ to $O(N_i+N_j)$, where N_i and N_j is the number of the dipoles in group i and j, respectively.

5 Numerical Results and Discussion

The generalized minimum residual methods (GMRES) iterative solver is employed to obtain an identical residual error which is smaller or equal to 0.001. All the simulations are performed on a personal computer with the Intel(R) Pentium(R) Dual-Core CPU E2200 with 2.0 GHz (only one core is used) and 2.0 GB RAMf.

As the first example, we consider a plane wave scattering from a chiral cube of side length $0.2\lambda_0$. The chiral cube is characterized by a relative chirality ξ_r, where $\mathrm{j}\xi_r=\xi/\sqrt{\varepsilon_r\mu_r}$, and $\xi=-\zeta$. The relative permittivity, permeability and chirality are $\varepsilon_r=9$, $\mu_r=1$, and $\xi_r=0.0, 0.3, 0.5$, respectively. This body is illuminated by a plane electromagnetic wave from $\theta=0°$. The cube is divid-

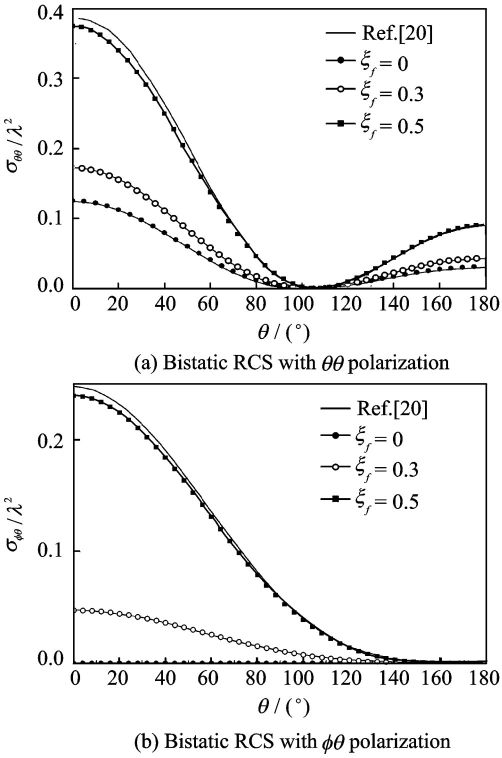

Fig. 1 Bistatic RCS of chiral cube

ed into 4 023 volumetric cells with an average edge length of $0.025\lambda_0$, and the total number of unknowns is 16 860. All the unknowns are divided into 261 nonempty groups and the size of each group is 0.04λ for using the FDM. The normalized $\theta\theta$ and $\varphi\theta$ polarization bistatic RCS of the chiral cube shown in Fig. 1 are compared to those from Ref. [20] and good agreements are observed. The CPU time, memory requirement and iterations when $\xi_r = 0.5$ are shown in Table 1. However, it is impossible to solve this problem using the conventional MoM and EDM method for insufficient memory.

Table 1 Total CPU time, memory cost and iterations of RCS solutions for FDM

Object	Time/s	RAM/MB	Iteration
Cube ($\xi_r = 0.5$)	1 628	291	66
Cylinder ($\Omega = 0.5$)	1 601	363	20
Spheres	9 519	1 060	80

In the second example, we calculate plane wave scattering from an omega cylinder. The radius and height of the finite circular cylinder are $a = 0.5\lambda$ and $h = 0.2\lambda$, respectively. It is known that omega materials are a special type of bi-anisotropic media whose constitutive tensors are in the form as follows

$$\bar{\bar{\boldsymbol{\varepsilon}}}_r = \begin{bmatrix} \varepsilon_1 & 0 & 0 \\ 0 & \varepsilon_2 & 0 \\ 0 & 0 & \varepsilon_3 \end{bmatrix}, \quad \bar{\bar{\boldsymbol{\mu}}}_r = \begin{bmatrix} \mu_1 & 0 & 0 \\ 0 & \mu_2 & 0 \\ 0 & 0 & \mu_3 \end{bmatrix}$$

$$\bar{\bar{\boldsymbol{\xi}}} = \begin{bmatrix} 0 & 0 & 0 \\ \mathrm{j}\Omega & 0 & 0 \\ 0 & 0 & 0 \end{bmatrix}, \quad \bar{\bar{\boldsymbol{\zeta}}} = \begin{bmatrix} 0 & -\mathrm{j}\Omega & 0 \\ 0 & 0 & 0 \\ 0 & 0 & 0 \end{bmatrix} \tag{41}$$

where $\varepsilon_1 = 2, \varepsilon_2 = 3, \varepsilon_3 = 2, \mu_1 = 1.2, \mu_2 = 1.2, \mu_3 = 1.0, \Omega = 0.0, 0.5, 1.0$. The cube is divided into 6 950 volumetric cells with an average edge length of 0.06λ, and the total number of unknowns is 29 274. Totally 589 nonempty groups with the size of $0.08\lambda_0$ are obtained. The CPU time, memory requirement and iterations when $\Omega = 0.5$ are shown in Table 1. The $\theta\theta$ polarized bistatic RCS for a normally incident plane wave are calculated. Results shown in Fig. 2 are compared to those from Ref. [6] and good agreements are observed.

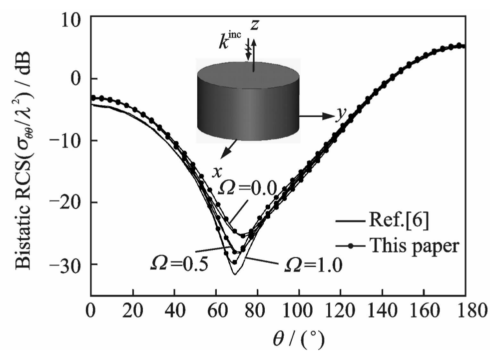

Fig. 2 $\theta\theta$ polarized bistatic RCS from an omega cylinder

In the last example, we consider spheres with different constitutive parameters to demonstrate the versatility of our code in solving bi-anisotropic problems. There are four spheres along the x direction. The radiuses of the spheres are $0.2\lambda_0$ and the distance between them is $0.5\lambda_0$. The first one is a gyroelectric sphere with $\bar{\bar{\boldsymbol{\varepsilon}}}_r = \begin{bmatrix} 2.5 & & \mathrm{j} \\ -\mathrm{j} & 2.5 & 0 \\ 0 & 0 & 1.5 \end{bmatrix}$. The second one is a gyromagnetic sphere with $\bar{\bar{\boldsymbol{\mu}}}_r = \begin{bmatrix} 2.5 & \mathrm{j} & 0 \\ -\mathrm{j} & 2.5 & 0 \\ 0 & 0 & 1.5 \end{bmatrix}$. The third one is a chiral sphere with $\bar{\bar{\boldsymbol{\varepsilon}}}_r = 1.5\bar{\bar{\boldsymbol{I}}}$, $\bar{\bar{\boldsymbol{\mu}}}_r = 1.5\bar{\bar{\boldsymbol{I}}}$, $\bar{\bar{\boldsymbol{\xi}}} = -\bar{\bar{\boldsymbol{\zeta}}} = -0.2\bar{\bar{\boldsymbol{I}}}_j$. The last one is a

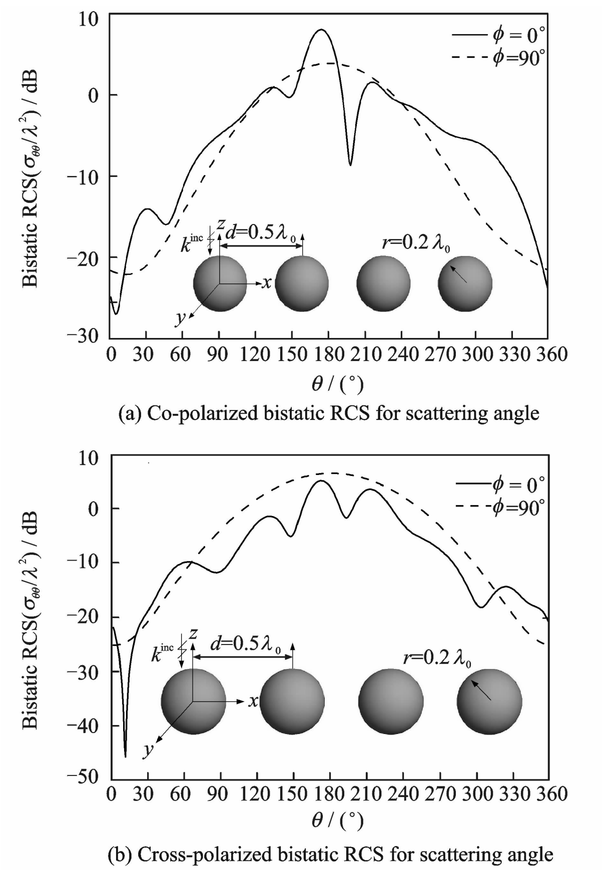

Fig. 3 Bistatic RCS of spheres

Faraday chiral sphere with $\bar{\bar{\boldsymbol{\varepsilon}}}_r = \begin{bmatrix} 2.5 & \mathrm{j} & 0 \\ -\mathrm{j} & 2.5 & 0 \\ 0 & 0 & 1.5 \end{bmatrix}$, $\bar{\bar{\boldsymbol{\mu}}}_r = \begin{bmatrix} 2.5 & \mathrm{j} & 0 \\ -\mathrm{j} & 2.5 & 0 \\ 0 & 0 & 1.5 \end{bmatrix}$, $\bar{\bar{\boldsymbol{\xi}}} = -\bar{\bar{\boldsymbol{\zeta}}} = -0.2\bar{\bar{\boldsymbol{I}}}_j$. The configuration of the spheres is shown in Fig. 3. The spheres are discretized into 14 696 tetrahedrons. The total number of unknowns is 61 038. Totally 2 635 nonempty groups with the size of $0.04\lambda_0$ are obtained. Fig. 3 shows the bistatic RCS of the spheres for a normally incident plane wave. We have computed both co-polarized and cross-polarized RCS for scattering angle $\phi = 0°, 90°$, respectively. From these figures, we can see that for $\sigma_{\theta\theta}$ and $\sigma_{\phi\theta}$, the results in $\phi = 0°$ plane are larger than those in $\phi = 90°$ plane. For the RCS, the results have many valleys in $\phi = 0°$ plane, while they are smooth in $\phi = 90°$ plane. The cross-polarized RCS for the bi-anisotropic object can not be ignored. The CPU time, memory requirement and iterations are shown in Table 1. From Table 1, we can see that the FDM can save the memory requirement and speed up the solution process significantly.

6 Conclusions

VIE based on the volume equivalence principle has been formulated for scattering from bi-anisotropic bodies with arbitrary shape. Then the FDM are extended to solve the problem. The application of FDM can reduce the memory requirement and improve computational efficiency significantly. Numerical examples are presented to illustrate the accuracy and versatility of the proposed method. The obtained results also show that the cross-polarized bistatic RCS for bi-anisotropic materials can not be ignored.

References:

[1] Serdyukov A, Semchenko I, Tretyakov S, et al. Electromagnetics of bi-anisotropic materials: Theory and applications [M]. New York: Gordon and Breach, 2001.

[2] Gao L, Fung T H, Yu K W, et al. Electromagnetic transparency by coated spheres with radial anisotropy [J]. Physical Review E, 2008, 78: 046609/1-046609/11.

[3] Kriegler C E, Rill M S, Linden S, et al. Bianisotropic photonic metamaterials[J]. IEEE J Sel Topics Quantum Electron, 2010, 16(2): 367-375.

[4] Zebiri C, Lashab M, Benabdelaziz F. Rectangular microstrip antenna with uniaxial bi-anisotropic chiral substrate-superstrate [J]. IET Microw Antennas Propag, 2011, 5(1): 17-29.

[5] Demir V, Elsherbeni A Z, Arvas E. FDTD formulation for dispersive chiral media using the Z transform method [J]. IEEE Trans Antennas Propag, 2005, 53(10): 3374-3384.

[6] Zhang Y, Wei X, Li E. Electromagnetic scattering from three-dimensional bianisotropic objects using hybrid finite element-boundary integral method [J]. Journal of Electromagnetic Waves and Applications, 2004, 18(11): 1549-1563.

[7] Kobidze G, Shanker B. Integral equation based analysis of scattering from 3-D inhomogeneous anisotropic bodies [J]. IEEE Trans Antennas Propag, 2004, AP-52(10): 2650-2658.

[8] Mei C, Hasanovic M, Lee J K, et al. Electromagnetic scattering from an arbitrarily shaped three-dimensional inhomogeneous bianisotropic body [J]. Piers Online, 2007, 3(5): 680-684.

[9] Hu L, Li J L W, Yeo T S. Analysis of scattering by large inhomogeneous bi-anisotropic objects using AIM[J]. Progress In Electromagnetics Research, 2009, 99: 21-36.

[10] Song J M, Lu C C, Chew W C. Multilevel fast multipole algorithm for electromagnetic scattering by large complex objects[J]. IEEE Trans Antennas Propag, 1997, 45(10): 1488-1493.

[11] Pan X M, Cai L, Sheng X Q. An efficient high order multilevel fast multipole algorithm for electromagnetic scattering analysis [J]. Progress In Electromagnetics Research, 2012, 126: 85-100.

[12] Zhu Xiuqin, Geng Youlin, Wu Xinbao. Application of MOM-CGM-FFT method to scattering from three-dimensional anisotropic scatterers [J]. Chinese Journal of Radio Science, 2002, 17(3): 209-215. (in Chinese)

[13] Hu L, Li L W, Yeo T S. Analysis of scattering by large inhomogeneous bi-anisotropic objects using AIM[J]. Progress In Electromagnetics Research, 2009, 99: 2-36.

[14] Yuan J D, Niu Z Y, Li Z, et al. Electromagnetic scattering by arbitrarily shaped PEC targets coated with anisotropic media using equivalent dipole-moment method [J]. J Infrared Milli Terahz Waves, 2010, 31(6):744-752.

[15] Deng X Q, Gu C Q, Zhou Y G. Electromagnetic scattering by arbitrary shaped three-dimensional conducting objects covered with electromagnetic anisotropic materials [J]. Applied Computational Electromagnetics Society Journal, 2011, 26(11): 886-892.

[16] Chen X L, Gu C Q, Niu Z Y, et al. Fast dipole method for electromagnetic scattering from perfect electric conducting targets [J]. IEEE Trans Antennas Propag, 2012, 60(2): 1186-1191.

[17] Chen X L, Li Z, Niu Z Y, et al. Analysis of electromagnetic scattering from PEC targets using improved fast dipole method [J]. Journal of Electromagnetic Waves and Applications, 2011, 25(16): 2254-2263.

[18] Deng Xiaoqiao, Li Zhuo, Niu Zhenyi. Fast calculation method for RCS of electromagnetic anisotropic dielectric [J]. Journal of Nanjing University of Aeronautics & Astronautics, 2012, 44(4): 570-574. (in Chinese)

[19] Schaubert D H, Wilton D R, Glisson A W. A tetrahedral modeling method for electromagnetic scattering by arbitrarily shaped inhomogeneous dielectric bodies [J]. IEEE Trans Antennas Propag, 1984, 32 (1): 77-85.

[20] Worasawate D, Mautz J R, Arvas E. Electromagnetic scattering from an arbitrarily shaped three-dimensional homogeneous chiral body [J]. IEEE Trans Antennas Propag, 2003, 51(5): 1077-1084.

(Executive editor: Xu Chengting)